AIAA 80-0795R

Aeroelastic Tailoring of Forward Swept Composite Wings

Terrence A. Weisshaar*
Purdue University, West Lafayette, Ind.

A set of closed-form solutions to idealized static aeroelastic problems is presented. These solutions describe the effects of fibrous composites on flexible lifting surface divergence, lift effectiveness, and spanwise center-of-pressure location. Several examples illustrate the ability of aeroelastic tailoring to modify spanwise center-of-pressure location. Additional examples, using data generated from a matrix method of analysis, show that tailoring for forward swept wing divergence is likely to be effective out to relatively high aspect ratios and that lateral control effectiveness can be enhanced considerably by fibrous composite tailoring.

Nomenclature

a_0 = sectional lift-curve slope
c = wing chordwise dimension (Fig. 1)
d = offset between wing section center of mass (c.m.) and reference axis, positive when c.m. is forward of the reference axis
e = offset between section aerodynamic center and the reference axis (Fig. 1)
g = ratio K/GJ
h = reference axis deflection, positive upward
k = ratio K/EI
K = bending/torsion coupling parameter, Eq. (A13)
ℓ = wing semispan dimension, measured along the reference axis
= wing semispan dimension, measured perpendicular to the fuselage
q = dynamic pressure
q_D = divergence dynamic pressure for a 30 deg forward swept wing with all tailoring fibers θ oriented parallel to the reference axis direction
r = coordinate measured along the swept reference axis (Fig. 1)
y = coordinate measured along an axis perpendicular to the fuselage
Δy^* = change in the spanwise location of the wing center of pressure, measured along the y axis, divided by ℓ
$\Delta \bar{y}^*$ = change in the spanwise location of the center of pressure, measured along the $\bar{y}$ axis, divided by $\bar{\ell}$
z = vertical distance to an individual lamina, measured perpendicular to the laminate mid-surface, positive upward
η = $1 - y/\ell$

Introduction

THE optimal utilization of structural material in aircraft design has always been an objective of designers. New performance objectives, together with material and manufacturing constraints, have led to radical changes in the shape of the airplane over the last three-quarters of the century. The recent introduction of modern composite materials into the realm of aircraft design has led to new airframe design concepts and also to the re-evaluation of older concepts as well. Specifically, the availability of composite materials has renewed interest in forward swept wing performance and design.[1,2]

Because of the modern-day requirement for high speed with a lightweight structure, close attention must be given to the aeroelastic performance of a proposed design. Recently, a large amount of research effort has been directed toward the least-weight optimization of practical aircraft structures with aeroelastic constraints. The aeroelastic optimization of structures composed of laminated composites is commonly referred to as aeroelastic tailoring, a term that is certainly appropriate considering the ribbon or cloth-like appearance of the precured composite material. References 3 and 4 will provide the unfamiliar reader with a comprehensive review of optimization concepts and papers related to aeroelastic tailoring.

There are in existence several computerized methods to determine the distribution and orientation of fibrous composite materials to obtain optimal aeroelastic performance of lifting surfaces. In addition, tailoring of actual wings has been accomplished. However, the present author feels that a need exists to document some of the more important consequences and benefits of the use of aeroelastic tailoring on swept wing structures. This need is perceived to exist not only because of the added material design dimension of fiber orientation and ply lay-up, but because of the absence of documentation of fundamental principles related to composite wing aeroelasticity.

To partially remedy the lack of a fundamental data base in this area, this paper will illustrate several effects of laminate lay-up and fiber orientation upon aeroelastic divergence, wing load redistribution, and lateral control effectiveness of both sweptback and sweptforward wings. To accomplish these objectives, two theoretical models were formulated. The first of these models uses laminated plate theory, together with elementary strip theory airloads, to develop the spanwise lift redistribution problem for a uniform-planform swept wing. The second model employs a more general representation of the laminated wing structure, together with a realistic discrete-element aerodynamic loading, to study the lift redistribution, lift effectiveness, and aileron effectiveness problem for composite wings.

Subcritical Static Aeroelastic Deformation of a Uniform Planform Wing

The static aeroelastic behavior of a metallic wing with a uniform planform is examined in detail by Diederich and Foss.[5] In their report they observe that the aeroelastic deformation of the wing results in a change in the spanwise distribution of the aerodynamic loads. This change may have a pronounced effect upon such important items as lift-curve slope of a lifting surface and the distribution of stresses within the support structure. In addition, for swept wings,

Presented as Paper 80-0795 at the AIAA/ASME/ASCE/AHS 21st Structures, Structural Dynamics and Materials Conference, Seattle, Wash., May 12-14, 1980; submitted July 12, 1980; revision received Feb. 23, 1981.

*Associate Professor, School of Aeronautics and Astronautics. Member AIAA.

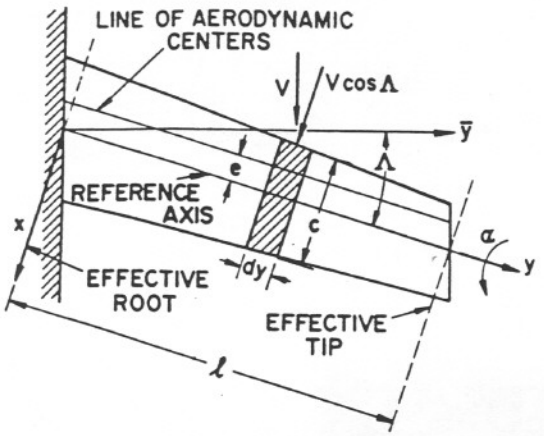

Fig. 1 Idealized wing planform geometry.

aeroelastic deformation will lead to changes in the longitudinal position of the center of pressure and affect the stability of the aircraft. It is well known that the static aeroelastic behavior of the wing may significantly influence the design of the wing structure and aircraft control system.

Because of the potential influence of static aeroelasticity on swept wing design, it is useful to assess the degree to which modern composite materials can modify static aeroelastic behavior. Throughout this paper, attention will be focused on constant weight configurations. The parameter to be varied will be the fiber orientation of a certain percentage of the laminated structure.

To focus maximum attention upon the effect of laminated materials on static aeroelasticity of lifting surfaces, the simplified approach of Ref. 5 will be used. To study the deformation of a uniform-planform wing, the differential equations of equilibrium, in terms of bending and torsional deformations of a slender swept wing, were formulated by considering the aerodynamic loads to act upon chordwise segments of the wing perpendicular to the wing reference axis, as shown in Fig. 1. The structural model for the wing assumes the loads to be carried by a box-beam arrangement in which laminated composite plates form the upper and lower face sheets of the wing box. A reference axis, labeled as the y axis in Fig. 1, is located equidistant between the front and rear edges of the box beam and lies in the geometric midplane of the box, halfway between the upper and lower surfaces of the cover sheets.

Reference 6 describes in detail the theoretical development of the laminated-composite, box-beam structural model. The governing equations for the deformation of such a model under aerodynamic load are reproduced in the Appendix. These equations contain several parameters that must be discussed to understand fully the results to follow.

The laminated box-beam model is characterized by three parameters, *EI*, *GJ*, and *K*. These parameters represent the beam bending stiffness, torsional stiffness, and the bending-torsion coupling parameter, respectively. Algebraic expressions for these parameters are reproduced in the Appendix. These parameters closely resemble those developed in laminated plate bending theory (cf. Ref. 7). *EI*, *GJ*, and *K* are functions of the box-beam geometry and the material properties and orientation of the various laminae in the cover-sheet laminates. The model recognizes that, from a fabrication standpoint, the laminates themselves should be symmetrical in their lay-up, but the top and bottom cover sheets do not necessarily need to be identical. In this latter case, the box beam would be unsymmetrical.

The wing deflections are those of a moderate-to-high-aspect-ratio wing under the action of strip theory airloads. This representation of the loads is not as inaccurate as one might think, since the two-dimensional sectional lift-curve slope used in this model may be adjusted empirically to reflect the influence of sweep and finite-span effects. The wi deformation consists of an upward bending deflection of t reference axis $h(y)$ and a nose-up twisting about the y a $\alpha(y)$.

The local angle of attack due to deflections $h(y)$ and $\alpha($ is denoted as α_e, and is defined as:

$$\alpha_e = \alpha - \frac{dh}{dy}\tan\Lambda$$

The equations for the static response of the untwist uniform-planform wing under the action of strip theory lo and gravity loads are derived in Ref. 6 using methods adap from Ref. 5. The features of these equations are noted in discussion to follow.

The character of the external loads is contained in a c stant f_2 written as:

$$f_2 = \left(\frac{g-\tan\Lambda}{1-kg}\right)\left[\frac{qc\ell^3 c_l'\cos^2\Lambda}{EI} - \frac{nw\ell^3}{EI}\right]$$

In Eq. (2), the term c_l' corresponds to the two-dimensional coefficient for rigid wing sections perpendicular to reference axis. The parameters k and g are nondimensio bending-torsion coupling ratios

$$k = K/EI$$

$$g = K/GJ$$

The distributed inertia load per unit length nw is for a w of weight w pounds per unit length operating at a load fac n, while q represents the flight dynamic pressure.

Two aeroelastic parameters appear in the composite sw wing static aeroelastic problem. These parameters, terme and b, are defined as follows:

$$a = \left(\frac{qce\ell^2 a_0\cos^2\Lambda}{GJ}\right)\left(\frac{1-k\tan\Lambda}{1-kg}\right)$$

$$b = \left(\frac{qc\ell^3 a_0\cos^2\Lambda}{EI}\right)\left(\frac{\tan\Lambda-g}{1-kg}\right)$$

In Eqs. (5) and (6), a_0 is the two-dimensional lift-curve sl of a section perpendicular to the reference axis. The solut for $\alpha_e(\eta)$, where $\eta = 1 - y/\ell$, is given as:

$$\alpha_e(\eta) = \frac{f_2}{b}\left[1 - \frac{f_3(\eta)}{f_3(1)}\right]$$

The function $f_3(\eta)$ is defined in terms of parameters β an that are functions of a and b

$$f_3(\eta) = \left[\frac{4\beta^2}{9\beta^2+\gamma^2}\right]e^{-2\beta\eta} + e^{\beta\eta}\left[\left(\frac{5\beta^2+\gamma^2}{9\beta^2+\gamma^2}\right)\cos\gamma\eta + \left(\frac{3\beta^3-\beta\gamma^2}{9\beta^2\gamma+\gamma^3}\right)\right]\sin\gamma\eta$$

where

$$\beta = -\frac{1}{2}(c_1+c_2)$$

$$\gamma = \frac{\sqrt{3}}{2}(c_1-c_2)$$

and

$$c_1 = \left[\frac{b}{2} + \sqrt{\frac{b^2}{4}+\frac{a^3}{27}}\right]^{1/3}$$

$$c_2 = \left[\frac{b}{2} - \sqrt{\frac{b^2}{4}+\frac{a^3}{27}}\right]^{1/3}$$

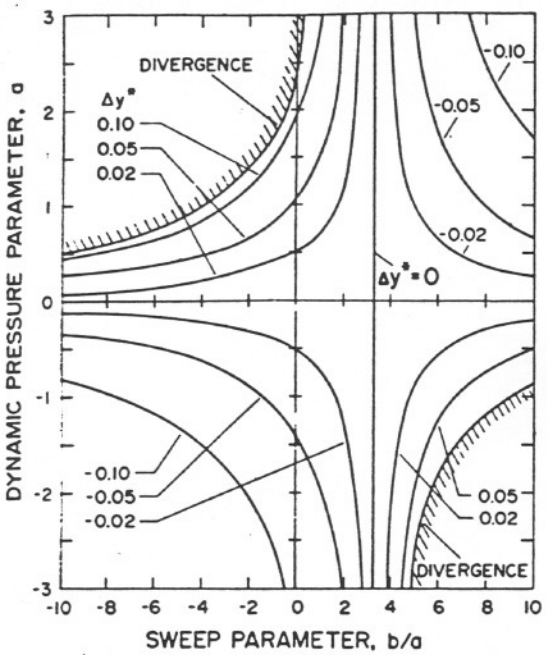

Fig. 2 Effect of the pressure parameter a and sweep parameter b upon spanwise center of pressure change Δy^*.

Equation (7) provides information necessary to obtain a closed-form solution for the ratio between the total lift developed by a flexible composite wing and the lift developed by a similar inflexible wing. With the strip theory approximation, the net lift on the rigid wing is

$$L_r = qcc_l'\ell\cos^2\Lambda - nw\ell \tag{13}$$

The net lift on the flexible wing is

$$L = L_r + \int_0^\ell (qca_0\cos^2\Lambda)\alpha_e\,dy \tag{14}$$

The combination of Eqs. (7), (13), and (14) yields the expression for the flexible-to-rigid wing lift ratio:

$$\frac{L}{L_r} = \frac{-2\beta\gamma e^{-2\beta} + 2\beta\gamma e^{\beta}\cos\gamma + (3\beta^2+\gamma^2)e^{\beta}\sin\gamma}{4\beta^2 e^{-2\beta} + e^{\beta}[(5\beta^2+\gamma^2)\cos\gamma + (3\beta^2-\beta\gamma^2)\sin\gamma]} \tag{15}$$

Equation (15) is an expression for the lift effectiveness of the wing. Note that, when the denominator becomes zero, the wing will encounter a clamped wing divergence instability.

The ratio of the flexible wing bending moment about the wing effective root to that for the rigid wing is found to be:

$$\frac{M}{M_r} = 2\left[\frac{\gamma e^{-2\beta} + e^{\beta}(-\gamma\cos\gamma + 3\beta\sin\gamma)}{4\beta^2\gamma e^{-2\beta} + e^{\beta}[(5\beta^2\gamma+\gamma^3)\cos\gamma + (3\beta^3-\beta\gamma^2)\sin\gamma]}\right] \tag{16}$$

The expression for the twisting moment ratio is identical to that calculated for the ratio L/L_r. The spanwise center of pressure y_{CP}, measured along the reference axis, is obtained by combining Eqs. (15) and (16) and reads as follows:

$$y_{CP} = \frac{\ell}{2}\left(\frac{M}{M_r}\right)\left(\frac{L_r}{L}\right) \tag{17}$$

Influence of Flexibility on Wing Spanwise Center of Pressure

The change in the spanwise position of the center of pressure, due to wing flexibility, affects both the longitudinal stability of the aircraft and the stresses at the wing root. Equation (17) may be used to compute the *change* in the spanwise location of the center-of-pressure position along the swept reference axis. Reference 5 presents a study of this change for uniform-planform metallic wings as a function of two aeroelastic parameters related to dynamic pressure and wing sweep angle. The present study presents similar results by suitably redefining parameters used in Ref. 5 to reflect the presence of a laminated beam structure. The two aeroelastic parameters to be used are the parameter a, defined in Eq. (5), and the ratio b/a, defined as follows:

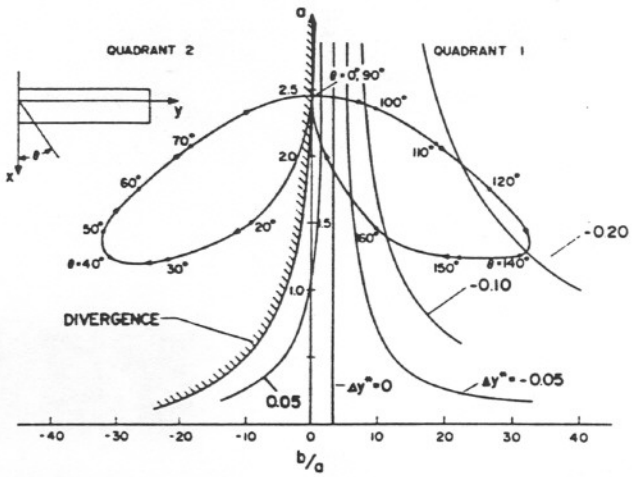

Fig. 3 Effect of fiber orientation θ upon spanwise center-of-pressure change Δy^* for a uniform-planform wing at zero sweep and fixed dynamic pressure.

$$\frac{b}{a} = \left(\frac{\ell}{e}\right)\left[\frac{\tan\Lambda - g}{1 - k\tan\Lambda}\right]\left[\frac{GJ}{EI}\right] \tag{18}$$

In Ref. 5, where k and g are zero, the parameter a is referred to as the dynamic pressure parameter, while b/a is termed the sweep parameter. Figure 2 shows the influence of these parameters upon the movement of the center of pressure (CP) along the swept reference axis shown in Fig. 1. The parameter Δy^* is equal to $\Delta y_{CP}/\ell$, so that positive Δy^* corresponds to an outward CP movement while, conversely, inboard CP movement is characterized by negative values of Δy^*.

Labelling the upper right quadrant of Fig. 2 as quadrant 1 and numbering the other quadrants consecutively counterclockwise, we see that values of a and b/a lying in quadrant 1 correspond to situations for which divergence is very unlikely to occur. In addition, the center-of-pressure movement is inboard for values of b/a greater than about 4.

In quadrant 2, clamped wing divergence is very likely, except for wings falling into a very small region of a and b/a values. In addition, shifts in the CP location are outboard so that unfavorable effects of aeroelasticity upon wing stresses may be expected in this region. In quadrant 3 divergence is impossible, while in quadrant 4 divergence may be possible for certain combinations of a and b/a.

Reference 5 notes that subsonic, metallic sweptback wings ($k=g=0$) are described by values a and b/a lying in the first quadrant, while subsonic, metallic sweptforward wings fall into quadrant 2. For the parameter a to be negative for a metallic wing, the chordwise aerodynamic center must lie behind the wing elastic axis, a situation usually associated with supersonic flight. Quadrant 3 illustrates sweptback metallic wing behavior in the supersonic flight regime, while quadrant 4 corresponds to metallic sweptforward wing behavior at supersonic speeds.

When the wing is constructed of composite materials, the likely effect of sweep on aeroelastic behavior is not as clear as

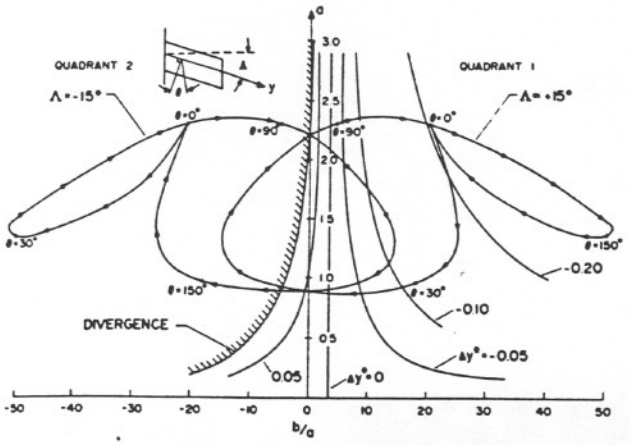

Fig. 4 Effect of fiber orientation θ upon the spanwise center of pressure change Δy^* for a uniform-planform wing at two sweep angles and a fixed dynamic pressure.

it is for metallic wings. The elastic coupling between bending and torsion introduces a new parameter into the definitions of a and b/a. For a particular value of wing sweep angle Λ and dynamic pressure, the values of a and b/a may be modified by tailoring of the composite laminate. This modification is illustrated by an example case discussed in the next section.

Example Case

To illustrate the potential effect of tailoring laminate fibers for static aeroelastic performance, an example wing was chosen. The wing has a constant chord and uniform elastic properties along the span. The laminated wing box-beam structure itself has a total laminate thickness/box-beam depth ratio of 1/10. The upper and lower cover sheets are identical: they are composed of graphite-epoxy with 10% of the laminate fibers oriented along the x axis (see Fig. 1), 25% along the ± 45 deg directions (with respect to the y axis), and 65% at a variable angle θ measured with respect to the x axis of the wing.

The dynamic pressure q chosen for this illustration corresponds to a value equal to the divergence q of an unswept wing with laminates for which the θ fibers are oriented along the reference axis ($\theta = 90$ deg). Since the stiffness parameters EI, GJ, and K are functions of the fiber angle θ, so too are a and b/a. Consider first Fig. 3, where a and b/a are plotted vs θ.

The plot or "tailoring loop" shown in Fig. 3 is symmetrical about the vertical axis. The curve is closed and exhibits a cusp where laminates with $\theta = 0$ and 90 deg have identical static aeroelastic behavior. It is seen that the effect of sweeping the θ fibers forward of the reference axis is to keep the wing static aeroelastic characteristics in quadrant 1, an effect similar to sweeping the entire wing rearward.

An additional feature of judicious fiber orientation is that the wing can be constructed so that it is aeroisoclinic at a certain dynamic pressure. By aeroisoclinic, it is meant that the flexible wing deforms in such a way that the spanwise center of pressure does not move, nor is the wing lift-curve slope changed from its rigid wing value. The aeroisoclinic behavior occurs at the fiber orientations given in Fig. 3 by the intersections of the vertical line marked $\Delta y^* = 0$ and the tailoring loop. These intersections occur for θ angles slightly greater than 90 and 170 deg.

Figure 4 shows a graph of a vs b/a for two uniform-property wings, one sweptback, the other sweptforward. The two loops are seen to be reflections of each other about the vertical line $b/a = 0$. For the 15 deg forward swept wing, a cusp point is located to the left of the $b/a = 0$ reference line. This point represents two wings, one with θ fibers at 0 deg and the other with θ near 73 deg. The 15 deg sweptback wing has a similar cusp when $\theta = 0$ and 107 deg. For both of these wings, it is possible to tailor the structure to achieve aeroisoclinic condition.

The two swept wings display dissimilar characteris Considering first the sweptback wing, the fiber orient region bounded approximately by 40 deg $< \theta <$ 90 de undesirable from the standpoint of CP movement possible divergence. Angles in the region 90 deg $\leq \theta \leq$ 180 may be undesirable from the standpoint of low lift fectiveness. The forward swept wing is governed by the posite rules. Fiber orientations in the 100 deg $< \theta <$ 140 region are desirable, because lift effectiveness is preserved high divergence speeds are obtained.

The effects of aeroelastic tailoring are bounded. Swee the wing beyond 15 deg of forward sweep further distort tailoring loop. The cusp point is moved further to the le that shown in Fig. 4 for $\Lambda = -15$ deg. Changing the fra of θ fibers within the laminate will also distort the loop will changes in wing geometry. Therefore, general conclus about the behavior of all laminated wings must be rea with caution.

Prospects for Tailoring of Forward Swept Wings

The previous discussion has focused on general behavio be expected from laminated composite wings. This sec will illustrate some characteristics of anisotropic swept w by examining specific wing planforms. From these res conclusions can be drawn about the probable effects of aspect ratio and taper ratio on the ability to tailor for swept composite wings.

The mathematical model to be used for the pre discussion differs from that described in the previous secti A flexibility matrix for a laminated beam is developed in 8 so that the equations of static equilibrium for the flex swept wing under load can be written in matrix form. Weissinger L method[9] is used to generate a matrix of ste state aerodynamic influence coefficients. Within assumptions of classical plate theory, these equations valid for a wing with a moderate-to-high aspect ratio and arbitrary planform. This approach, together with necessary equations, is described in detail in Ref. 8 and is repeated here.

The example wing structure consists of a constant-de box beam with thin, laminated cover sheets and rigid ver webs. The laminate construction is identical to that used in previous example. The wing planforms used in the pre example are both untapered and tapered, with the chord dimension linearly varying with distance from the wing ro

The Effect of Aspect Ratio on Divergence Tailorin

To illustrate the potential effect of wing aspect ratio on ability to tailor for divergence, two wings with differ aspect ratios were considered. Referring to Fig. 1, one w has $2\ell/c = 6$ while the other has $2\ell/c = 25$. Each wing ha reference axis swept forward 30 deg. The wings have differ aspect ratios, but some reasonable comparison between performance of the two wings must be made. For comparison, reference velocities V_{Rt}, different for each w are used to normalize the results. In the case where $2\ell/c$ the reference velocity V_{Rt} corresponds to the divergence sp of an *unswept reference wing* whose aerodynamic semispa 120 in. and whose chord is 40 in. The reference wing struc contains a laminate for which $\theta = 90$ deg so that the θ fil are oriented for maximum bending stiffness.

Considering the curve labelled $2\ell/c = 6$ in Fig. 5, it is that, at 30 deg of forward sweep, one may achiev divergence speed 37% larger than V_{Rt} by sweeping the θ fil forward of the reference axis about 20 deg. One might claim that a 37% improvement over V_{Rt} was possible with increase in weight. Of course, in fairness, it should mentioned that tailoring the unswept wing by reorienting

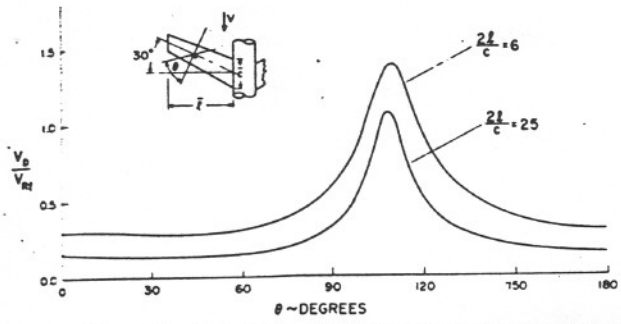

Fig. 5 Effect of laminate fiber orientation θ upon divergence speed V_D for two uniform-planform wings, each with the same chord but a different semispan ℓ (reference velocity V_{Rt} is unique to each wing).

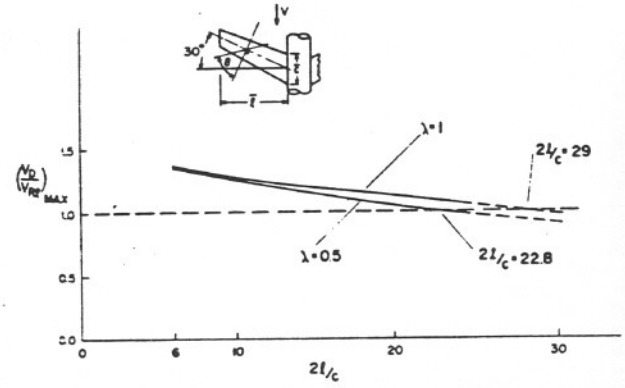

Fig. 6 Tailoring effectiveness parameter $(V_D/V_{Rt})_{max}$ plotted against the ratio $2\ell/c$ for two taper ratios λ (30 deg sweptforward wing).

fibers from the maximum bending stiffness position will produce an infinite divergence speed. However, the present comparison will still lead to a valuable and reasonable conclusion.

When $2\ell/c=25$ the results are not as dramatic. V_{Rt} in this second case is the divergence speed of an unswept wing with $2\ell/c=25$ and $\theta=90$ deg. The curve of V_D/V_{Rt} for $2\ell/c=25$ and $\Lambda=-30$ deg shows that an increase of 3% in V_D over V_{Rt} can be achieved by tailoring. This result indicates that aeroelastic tailoring is having difficulty coping with the reduced divergence speed caused by an increase in semispan. Anisotropic bending-torsion coupling is more pronounced for high-aspect-ratio wings than it is for low-aspect-ratio wings. This is true because a small change in wing twist occurring at some large distance from the wing root can cause a large bending deflection and vice versa.

A comparison of the relative change in V_D/V_{Rt} between the $\theta=90$ and 110 deg positions on each curve shows that at $2\ell/c=6$ the ratio of $(V_D/V_{Rt})_{max}$ to V_D/V_{Rt} at $\theta=90$ deg is of the order of 2, while the same ratio for $2\ell/c=25$ is about 6. The difference between the maximum values for the two curves in Fig. 5 results from the fact that an increase in span causes the divergence speed to decline sharply. At some point, even with the increased composite structure bending-torsion coupling, tailoring by fiber reorientation alone cannot cope with the adverse effect of wing span on divergence. In this case, additional structural material must be added and a weight penalty will occur.

Sobieski and coworkers at NASA/Langley Research Center[10] have observed that, on a specific design, aeroelastic tailoring can substantially reduce weight penalties for both forward and aft swept wings as long as the wing aspect ratios are not extreme. Figure 6 provides an indication of the "effectiveness" of aeroelastic tailoring of a forward swept wing with a divergence constraint for several aspect ratios. To provide a measure of effectiveness, the maximum values of

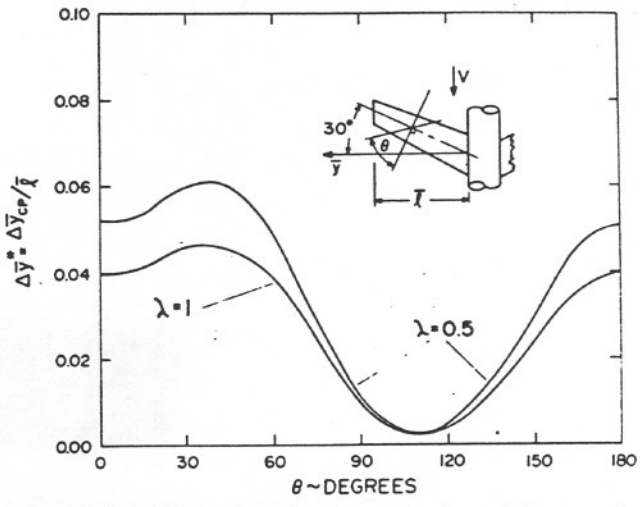

Fig. 7 Effect of fiber orientation θ upon the change in the spanwise center of pressure $\Delta\bar{y}^*$ for two taper ratios λ (30 deg sweptforward wing with $2\ell/c=6$ and fixed dynamic pressure, $q=0.2q_D^*$).

V_D/V_{Rt}, taken from plots similar to those in Fig. 5, are plotted in Fig. 6 for five different $2\ell/c$ ratios and two wing taper ratios λ where $\lambda=c_{tip}/c_{root}$. Where necessary, the curve connecting the five points was extrapolated, as indicated by the dashed lines. Values of $(V_D/V_{Rt})_{max}$ that lie below unity are defined to be those for which tailoring by fiber orientation is no longer effective. For $\lambda=1$ this point occurs at $2\ell/c=29$, while for $\lambda=0.5$ it is at $2\ell/c=22.8$.

Wing taper changes the values of the divergence speeds $(V_D)_{max}$ and the reference speeds V_{Rt}. The line corresponding to $(V_D/V_{Rt})_{max}$ for $\lambda=0.5$ lies below that for $\lambda=1$ in Fig. 6. This occurs because some area near the tip has been removed by taper and less wing structure is available to control divergence. While other measures of divergence effectiveness might be postulated, it seems fair to conclude that aeroelastic tailoring to satisfy a divergence constraint is still likely to be effective at fairly large aspect ratios and for small wing taper ratios.

The Effect of Flexibility on Spanwise Center-of-Pressure Position

Since fiber orientation of laminae within a box-beam laminate affects the stiffness properties of the wing, lamina fiber orientation will also determine the location of the spanwise position of the center of pressure of the aerodynamic loads at a given flight dynamic pressure. To illustrate the effects of wing aspect ratio, taper ratio, and fiber angle θ on spanwise center-of-pressure (CP) movement, a parameter $\Delta\bar{y}^*$ defined as

$$\Delta\bar{y}^* = (\bar{y}_{CPf} - \bar{y}_{CPr})/\bar{\ell} \tag{19}$$

is plotted vs the fiber angle θ of the tailored fibers. In Eq. (19) $\bar{y}_{CPf}$ is the spanwise location of the CP (measured perpendicular to the fuselage, see the insets of Figs. 7 and 8) on the flexible wing at any value of θ, while $\bar{y}_{CPr}$ is the spanwise CP value for an identical wing planform that does not deform.

The plot of $\Delta\bar{y}^*$ against θ is a function of dynamic pressure. For illustrative purposes, a reference value of dynamic pressure q_D^* was chosen to be equal to the divergence dynamic pressure of a 30 deg forward swept wing with similar taper, when $\theta=90$ deg. Note that q_D^* for the untapered wing ($\lambda=1$) is lower than q_D^* for the tapered wing.

Figure 7 demonstrates the range of values of CP movement possible through tailoring of the θ fibers for the 30 deg forward swept wing whose laminate properties were previously defined. For this figure, a value of q equal to 20% of q_D^* was

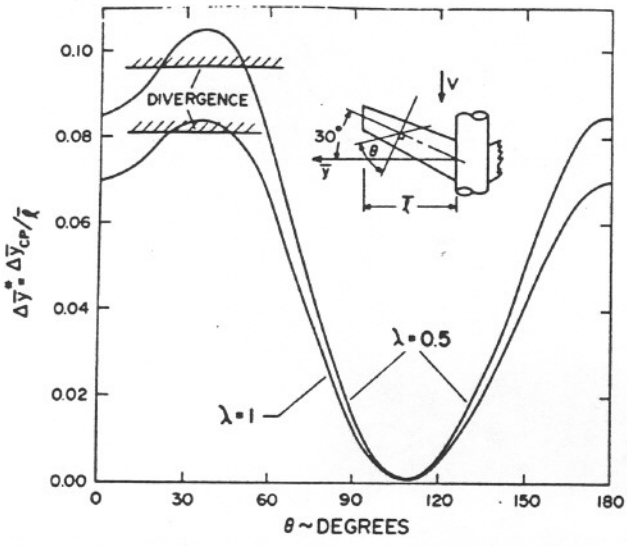

Fig. 8 Effect of fiber orientation θ upon the change in the spanwise center of pressure $\Delta\bar{y}^*$ for two taper ratios λ (30 deg sweptforward wing with $2\ell/c = 25$ and fixed dynamic pressure, $q = 0.2q_D^*$).

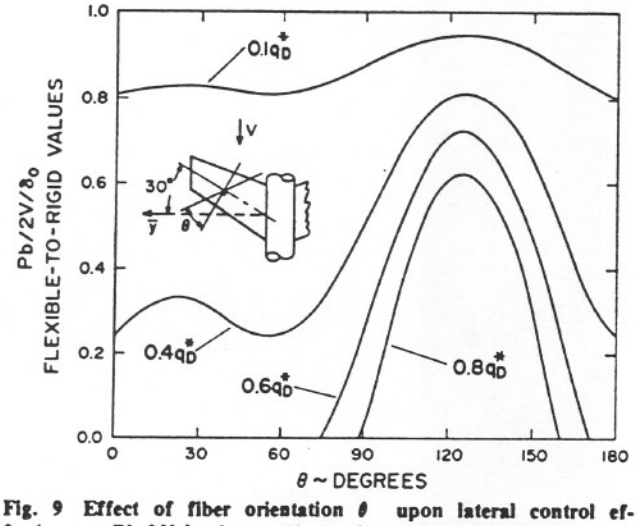

Fig. 9 Effect of fiber orientation θ upon lateral control effectiveness, $Pb/2V/\delta_\theta$, for a uniform-planform, 30 deg sweptforward wing at four different dynamic pressures (wing has 70% span ailerons and $2\ell/c = 6$).

chosen. The aeroisoclinic condition occurs if $\Delta\bar{y}^* = 0$. If the dynamic pressure were lower, aeroisoclinic conditions would occur near $\theta = 110$ deg.

Orientation of fibers in the aft quadrant is shown by Shirk and Griffin[4] to lead to a "wash-in" condition where upward bending leads to nose-up twist. Such a condition would be desirable on a sweptback wing, but not for forward sweep. Orienting fibers in the forward quadrant (90 deg $\leq \theta \leq$ 180 deg) creates a "wash-out" condition in which upward bending leads to nose-down twist, a desirable effect for sweptforward wings, but undesirable for sweptback wings. Relatively little forward sweeping of the fibers (on the order of 10-15 deg) beyond the reference axis position is necessary to achieve the maximum wash-out effect.

Figure 7 also shows that taper of the wing accentuates the range of movement of the CP with θ, but does not noticeably affect the minimum value of $\Delta\bar{y}^*$. It should be remembered that $\bar{y}_{CPr}$ for the tapered wing is less than that for the untapered wing.

In Fig. 8, the behavior of the center of pressure for a wing with an extreme aspect ratio ($2\ell/c = 25$) is presented. Once more, a dynamic pressure of 20% of q_D^* for each of the wings in question is used. The striking feature of Fig. 8, in contrast

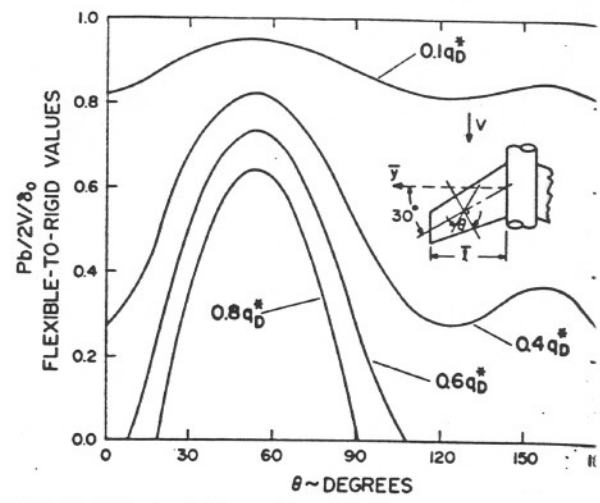

Fig. 10 Effect of fiber orientation θ upon lateral control fectiveness, $Pb/2V/\delta_\theta$, for a uniform-planform, 30 deg swept wing at four different dynamic pressures (wing has 70% span aile and $2\ell/c = 6$).

to Fig. 7, is the extreme outward movement of the CP wh lies in the aft quadrant. In fact, divergence occurs for a sr range of fiber angles. Divergence at this relatively small v of q occurs because the strong natural tendency of forw swept wings to wash-in due to bending is further exacerb by the wash-in feature of the anisotropic structure in region. Conversely, the effectiveness of the anisotr structure in negating the natural wash-in character of the w in the forward region of fiber orientation is clearly seer Fig. 8.

Tailoring for Lateral Control Effectiveness

In addition to requirements such as structural stabi (divergence) strength and longitudinal stability redistribution and CP location) the requirement for lat control effectiveness of an aircraft must be consider particularly for military aircraft. Since control effectiver of flexible swept wings depends upon coupling betw bending deformation and torsional deformation, structural coupling provided by laminate fiber orientation be shown to be significant.

A commonly accepted measure of aileron effectiveness the ratio $Pb/2V/\delta_0$, or simply $Pb/2V$, where:

P = steady-state roll rate, rad/s, caused by antisymmetrical aileron deflection
b = wing span, measured perpendicular to the fuselage
V = aircraft velocity
δ_0 = aileron deflection angle, rad

$Pb/2V$ is the helix angle traced out by the wing tip as it mov through space at a steady-state roll rate P. The aileron fectiveness is a function of flight speed, wing geomet stiffness, and aerodynamic characteristics such as c_{l_δ}, c_{l_α} and c_{l_β}.[11] When $Pb/2V$ becomes negative, the ailerons said to be reversed. Both military and civilian requiremer specify some measure of positive aileron effectiveness.

The example planform considered here is an untaper wing with 30 deg of forward sweep. The ratio $2\ell/c$ is Ailerons are located over 70% of the wing span in the regi between the wing tip and a position 30% outboard of the roc Aerodynamic parameters are $c_{l_\alpha} = 2\pi$, $c_{m_\delta} = -0.5$, a $c_{l_\beta} = 0.4$.

In Fig. 9, the value of $Pb/2V/\delta_0$ for the flexible win divided by the value computed for an identical but rigid win is plotted vs the fiber angle θ of 65% of the laminate for fo dynamic pressure conditions. As before, q_D^* is defined as t

divergence dynamic pressure of this 30 deg forward swept wing when $\theta = 90$ deg. When the θ fibers lie in the aft quadrant, the ailerons are seen to be highly prone to ineffectiveness. This occurs because the wash-in tendency of the anisotropic structure causes the wing to bend downward (and thus lose lift) when the wing is twisted downward by the aileron deflection. This downward twisting is a result of $c_{m\delta}$ being less than zero.

Aileron effectiveness of a forward swept wing is considerably enhanced by sweeping the θ fibers forward of the reference axis. Maximum effectiveness is reached near $\theta = 125$ deg (35 deg forward of the swept reference axis). This maximum aileron effectiveness occurs for a different value of θ than the value of θ associated with maximum divergence speed and will depend primarily upon the aileron characteristics and, to a lesser extent, upon q.

In Fig. 10, the behavior of an untapered 30 deg sweptback wing contrasts with that of the sweptforward wing. The dynamic pressure q_D^* used in Fig. 10 is identical to that used in Fig. 9, since the 30 deg sweptback wing will not diverge. The sweptback wing aileron effectiveness is almost, but not quite, the reflection (about the line $\theta = 90$ deg) of that shown in Fig. 9. Obviously, aileron effectiveness of the sweptback wing is enhanced when the fibers are in the aft quadrant and degraded when the θ fibers are in the forward quadrant. These results compare with those found in Ref. 12.

Conclusion

This paper has investigated several aspects of static aeroelastic tailoring of swept wings. In addition, several examples have illustrated the application of tailoring to forward swept wings. The proper orientation of a significant fraction of laminate structure fibers can markedly affect important static aeroelastic characteristics of the wing such as divergence speed, spanwise center of pressure, and aileron effectiveness. In some cases, an aeroisoclinic wing for a given dynamic pressure may be feasible. The concept of a tailoring loop has also been introduced to provide an indication of the design potential of a given laminate at a specified sweep angle and flight dynamic pressure.

Tailoring involving bending-torsion coupling is seen to be effective for high-aspect-ratio wings as well as low-aspect-ratio wings. However, more severe design requirements may negate this effectiveness if the span is too large. It appears that aeroelastic tailoring will be very effective in precluding large weight penalties due to divergence, for reasonable forward sweep, out to very high aspect ratios on the order of 20.

The fiber orientation position for maximizing lateral control effectiveness of a forward swept wing is near, but not at, the fiber position for maximizing divergence speed. Also important is the fact that the conclusions about the effect of fiber orientation on lateral control effectiveness of sweptforward wings are just the opposite to those for the sweptback wing.

Although the concept of tailoring for divergence has been proved in actual fabrication and test,[13] it remains to be seen how closely the above conclusions, based upon simplified models, compare to experimental results for a variety of parameters. In addition, the effects of fiber orientation on the flutter of forward swept wings is not yet well established and should be a fertile area of research.

Appendix

The governing equations of equilibrium for the wing shown in Fig. 1, with the assumption that structural deformation consists of a bending deflection $h(y)$ of the reference axis and a twisting rotation $\alpha(y)$ about that axis, are [note that $(\,)' = \mathrm{d}(\,)/\mathrm{d}y$]:

$$(EIh'' - K\alpha')'' = p(y) \tag{A1}$$

$$(-Kh'' + GJ\alpha')' = -t(y) \tag{A2}$$

The structural parameters EI, GJ, and K are the beam bending stiffness, torsional stiffness, and bending-torsion coupling parameter, respectively, derived in Ref. 6 and defined in Eqs. (A11-A21). The term $p(y)$ is the upward load per unit length measured along the y axis, while $t(y)$ is the nose-up torque per unit length also measured along the y axis. Aerodynamic strip theory is used to develop the following expressions:

$$p(y) = cc_l' q\cos^2\Lambda + qca_0\cos^2\Lambda(\alpha - \Gamma\tan\Lambda) - nw \tag{A3}$$

$$t(y) = qcec_l'\cos^2\Lambda + qc^2 c_{mac}\cos^2\Lambda - nwd + qcea_0(\alpha - \Gamma\tan\Lambda)\cos^2\Lambda \tag{A4}$$

Γ is the slope of the bending deformation, defined as $\Gamma = \mathrm{d}h/\mathrm{d}y$.

Equations (A1) and (A2) are coupled together by the dependence of the aerodynamic load upon the term $(\alpha - \Gamma\tan\Lambda)$ and by the structural coupling parameter K and its nondimensional counterparts $k = K/EI$ and $g = K/GJ$. These two equations can be combined to form a single equation in terms of a new variable α_e, defined as $\alpha_e = \alpha - \Gamma\tan\Lambda$.[5,8] This equation reads

$$\alpha_e'' + a\alpha_e' - b\alpha_e = f_1' - f_2 \tag{A5}$$

where

$$(\,)' = \mathrm{d}(\,)/\mathrm{d}\eta \qquad \text{and} \qquad \eta = (1 - y/\ell)$$

The parameters a, b, and f_2 are defined in Eqs. (2), (5), and (6), while

$$f_1 = \frac{1 - k\tan\Lambda}{1 - kg}\left[-\left(1 + \left(\frac{c}{e}\right)\left(\frac{c_{mac}}{c_l'}\right)\right) \times \left(\frac{qce\ell^2 c_l'\cos^2\Lambda}{GJ}\right) + \frac{nwd\ell^2}{GJ}\right] \tag{A6}$$

Boundary conditions are developed from the usual specification that α and Γ are zero at the effective wing root ($\eta = 1$), the bending moment and twisting moment are zero at the wing tip ($\eta = 0$), and the shear force at the wing tip is zero. These specifications lead to

$$\alpha_e(\eta = 1) = 0 \tag{A7}$$

$$\alpha_e'(\eta = 0) = 0 \tag{A8}$$

$$\alpha_e''(0) + a\alpha_e(0) = f_1(0) \tag{A9}$$

The solution to these equations for an untwisted uniform-planform wing whose pitch attitude is specified is detailed in Ref. 8. In this case, $f_1(\eta)$ and $f_2(\eta)$ are constants.

Stiffness Parameters

For a single orthotropic lamina, the relationship between membrane stresses and strains occurring in the beam laminae can be written, in matrix notation, as (cf. Refs. 7 and 14):

$$\begin{Bmatrix} \sigma_{yy} \\ \tau_{xy} \end{Bmatrix} = \begin{bmatrix} \bar{Q}_{22} & \bar{Q}_{26} \\ \bar{Q}_{26} & \bar{Q}_{66} \end{bmatrix} \begin{Bmatrix} \epsilon_{yy} \\ \gamma_{xy} \end{Bmatrix} \tag{A10}$$

The terms $\bar{Q}_{ij}$ are functions of the orthotropic material constants Q_{ij}, and the angle θ defining the orientation between the lamina principal axes and the box-beam reference axes. The lamina lies in a plane parallel to the x-y plane shown in Fig. 1; the angle θ is defined as a clockwise rotation from the x axis shown in Fig. 1.

The wing equations of equilibrium [Eqs. (A1) and (A2)] contain the expressions for the equivalent EI and GJ of the wing structure and also K, the bending-torsion coupling parameter. These terms are given by the expressions

$$EI = EI_0 - \frac{(B_{22})^2}{A_{22}} \tag{A11}$$

$$GJ = GJ_0 - \frac{(B_{33})^2}{A_{22}} \tag{A12}$$

$$K = K_0 - \frac{B_{22}B_{33}}{A_{22}} \tag{A13}$$

$$EI_0 = b\left[\sum_{i=1}^{N} \bar{Q}_{22}^{(i)} \beta_i\right] \tag{A14}$$

$$GJ_0 = b\left[\sum_{i=1}^{N} 4\bar{Q}_{66}^{(i)} \beta_i\right] \tag{A15}$$

$$K_0 = b\left[\sum_{i=1}^{N} 2\bar{Q}_{26}^{(i)} \beta_i\right] \tag{A16}$$

$$A_{22} = b\left[\sum_{i=1}^{N} \bar{Q}_{22}^{(i)} t_i\right] \tag{A17}$$

$$B_{22} = b\left[\sum_{i=1}^{N} \bar{Q}_{22}^{(i)} \delta_i\right] \tag{A18}$$

$$B_{33} = 2b\left[\sum_{i=1}^{N} \bar{Q}_{26}^{(i)} \delta_i\right] \tag{A19}$$

In Eqs. (A14-A19), b represents the chordwise width of the box beam measured perpendicular to the reference axis in Fig. 1. The summation in the equations extends over the N layers of composite material. The constants β_i and δ_i are defined in terms of lamina coordinates with respect to the middle surface. In terms of the lamina thickness t_i and lamina lower and upper position coordinates z_i and z_{i+1}, respectively, β_i and δ_i are defined as follows

$$\beta_i = \int_{z_i}^{z_{i+1}} z^2 dz = \tfrac{1}{3}(t_i^3 + 3t_i z_i^2 + 3z_i t_i^2) \tag{A20}$$

and

$$\delta_i = \int_{t_i} z dz = t_i(z_{i+1} + z_i)/2 \tag{A21}$$

The expressions for the wing stiffnesses presented above closely resemble those developed in Ref. 7 for plate bending. The reader is cautioned, however, that the present expressions assume that chordwise curvature is zero. This means that for an isotropic material the expression for EI in Eq. (A11) will have a factor of $1/(1-\mu^2)$ present, where μ is Poisson's ratio. This will lead to a slight (order of 10%) overestimate of the bending stiffness of a thin-plate wing with a rectangular solid cross section when compared to the usual definition of EI from beam bending theory. The difference introduced for composites is not significant.

Acknowledgments

The author gratefully acknowledges the support of this work by DARPA at Virginia Polytechnic Institute and State University under AFOSR Grant 77-3423D and AFFDL Contract F33615-79-C-3224.

References

[1] Krone, N. J. Jr., "Divergence Elimination with Advanced Composites," AIAA Paper 75-1009, 1975.

[2] Weisshaar, T. A., "Divergence of Forward Swept Composite Wings," *Journal of Aircraft*, Vol. 17, June 1980, pp. 442-448.

[3] Stroud, W. J., "Automated Structural Design with Aeroelastic Constraints: A Review and Assessment of the State of the Art," Paper presented at Structural Optimization Symposium, ASME Winter Meeting, New York, 1974.

[4] Shirk, M. H. and Griffin, K. E., "The Role of Aeroelasticity in Aircraft Design with Advanced Filamentary Composite Materials," Paper presented at Second Conference on Fibrous Composites in Flight Vehicle Design, Dayton, Ohio, May 1974.

[5] Diederich, F. W. and Foss, K. A., "Charts and Approximate Formulas for the Estimation of Aeroelastic Effects on the Loading of Swept and Unswept Wings," NACA TN 2608, Sept. 1951.

[6] Weisshaar, T. A., "Aeroelastic Stability and Performance Characteristics of Aircraft with Advanced Composite Sweptforward Wing Structures," AFFDL-TR-78-116, Sept. 1978.

[7] Tsai, S. W. and Hahn, H. T., *Introduction to Composite Materials*, Technomic Publishing Co., Inc., Westport, Conn., 1980.

[8] Weisshaar, T. A., "Forward Swept Wing Static Aeroelasticity," AFFDL-TR-79-3087, June 1979.

[9] Gray, W. L. and Schenk, K. L., "A Method for Calculating the Subsonic Steady-State Loading on an Airplane with a Wing of Arbitrary Plan Form and Stiffness," NACA TN 3030, July 1953.

[10] Sobieski, J., private communication, NASA/Langley Research Center, Nov. 1979.

[11] Bisplinghoff, R. L., Ashley, H., and Halfman, R. L., *Aeroelasticity*, Addison-Wesley, Reading, Mass., 1955, pp. 506-509.

[12] Lynch, R. W. and Rogers, W. A., "Aeroelastic Tailoring of Composite Materials to Improve Performance," *Proceedings of the AIAA/ASME/SAE 17th Structures, Structural Dynamics and Materials Conference*, 1976, pp. 61-79.

[13] Hertz, T. J., Shirk, M. H., Ricketts, R. H., and Weisshaar, T. A., "Aeroelastic Tailoring with Composites Applied to Forward Swept Wings," *Proceedings of the 5th DOD/NASA Conference on Fibrous Composites in Structural Design*, Jan. 1981.

[14] Jones, R. M., *Mechanics of Composite Materials*, McGraw-Hill Book Co., 1975, pp. 45-59.